Journal of Biomechanics 168 (2024) 112061

Contents lists available at ScienceDirect

Journal of Biomechanics

journal homepage: www.elsevier.com/locate/jbiomech

# The primary stability of a cementless PEEK femoral component is sensitive to BMI: A population-based FE study

Corine E. Post[a,*], Thom Bitter[a], Adam Briscoe[b], René Fluit[a,c], Nico Verdonschot[a,d], Dennis Janssen[a]

[a] Orthopaedic Research Laboratory, Radboud University Medical Center, Nijmegen, the Netherlands
[b] Invibio Ltd., Thornton Cleveleys, Lancashire, United Kingdom
[c] Faculty of Science and Engineering, University of Groningen, Groningen, the Netherlands
[d] Laboratory for Biomechanical Engineering, Faculty of Engineering Technology, University of Twente, Enschede, the Netherlands

ARTICLE INFO

*Keywords:*
Total knee arthroplasty
Polyetheretherketone
Cementless femoral knee component
Finite element simulation
Micromotion
Populationstudy

ABSTRACT

The use of polyetheretherketone (PEEK) for cementless femoral total knee arthroplasty (TKA) components is of interest due to several potential advantages, e.g. the use in patients with metal hypersensitivity. Additionally, the stiffness of PEEK closer resembles the stiffness of bone, and therefore, peri-prosthetic stress-shielding may be avoided. When introducing a new implant material for cementless TKA designs, it is important to study its effect on the primary fixation, which is required for the long-term fixation. Finite element (FE) studies can be used to study the effect of PEEK as implant material on the primary fixation, which may be dependent on patient factors such as age, gender and body weight index (BMI). Therefore, the research objectives of this study were to investigate the effect of PEEK vs cobalt-chrome (CoCr) and patient characteristics on the primary fixation of a cementless femoral component. 280 FE models of 70 femora were created with varying implant material and gait and squat activity. Overall, the PEEK models generated larger peak micromotions than the CoCr models. Distinct differences were seen in the micromotion distributions between the PEEK and CoCr models for both the gait and squat models. The micromotions of all femoral models significantly increased with BMI. Neither gender nor age of the patients had a significant effect on the micromotions. This population study gives insights into the primary fixation of a cementless femoral component in a cohort of FE models with varying implant material and patient characteristics.

## 1. Introduction

Primary fixation of the cementless femoral component is essential for bone ingrowth on and into the implant surface, which occurs a few weeks to months after total knee arthroplasty (TKA) procedure (Hofmann et al., 1997). This primary fixation is established by the compressive and shearing forces that are generated during the implantation of the press-fit components. Apart from the frictional properties of the implant surface, the primary fixation depends on the design and material of the femoral component. When introducing a new implant material for TKA designs, it is therefore important to study its effect on the primary fixation.

While cobalt-chrome (CoCr) alloy currently is the default material for cementless femoral TKA components, polyetheretherketone (PEEK-OPTIMA™) is of interest as the material has several potential advantages. One of the advantages of PEEK is that it can be used in patients with metal hypersensitivity. Moreover, the use of a non-metal TKA allows for easier analysis of the peri-prosthetic tissue with modalities such as MRI and CT in case of implant failure as metal artefacts will be avoided (Nishio et al., 2023). From a mechanical perspective, the stiffness of PEEK (3.7 GPa) closer resembles the stiffness of human bone that is replaced during the surgery compared to CoCr (210 GPa). Therefore, the potential peri-prosthetic stress-shielding may be reduced (de Ruiter et al., 2017; Rankin et al., 2016).

To study the effect of PEEK as an implant material on the primary fixation, finite element (FE) studies can be adopted to simulate micromotions at the implant – bone interface, which can be used to evaluate the ingrowth potential of press-fit implants. Previous FE studies on the cementless PEEK femoral component mainly focused on the analysis of a single femoral model with parametric variations (Post et al., 2022),

* Corresponding author at: Orthopaedic Research Lab 620, Geert Grooteplein Zuid 30, 6525 GA Nijmegen, the Netherlands.
*E-mail address:* corine.post@radboudumc.nl (C.E. Post).

https://doi.org/10.1016/j.jbiomech.2024.112061
Accepted 21 March 2024
Available online 24 March 2024

**Table 1**
Patient characteristics (n = 35).

| **Gender** | |
|---|---|
| M | N = 15 (43 %) |
| F | N = 20 (57 %) |
| **Age** in years, mean (range) | 62 (46 – 75) |
| **Height** in m, mean (range) | 1.72 (1.55 – 1.90) |
| **Weight** in kg, mean (range) | 78 (52 – 170) |
| **BMI** in kg/m$^2$, mean (range) | 26 (19 – 49) |

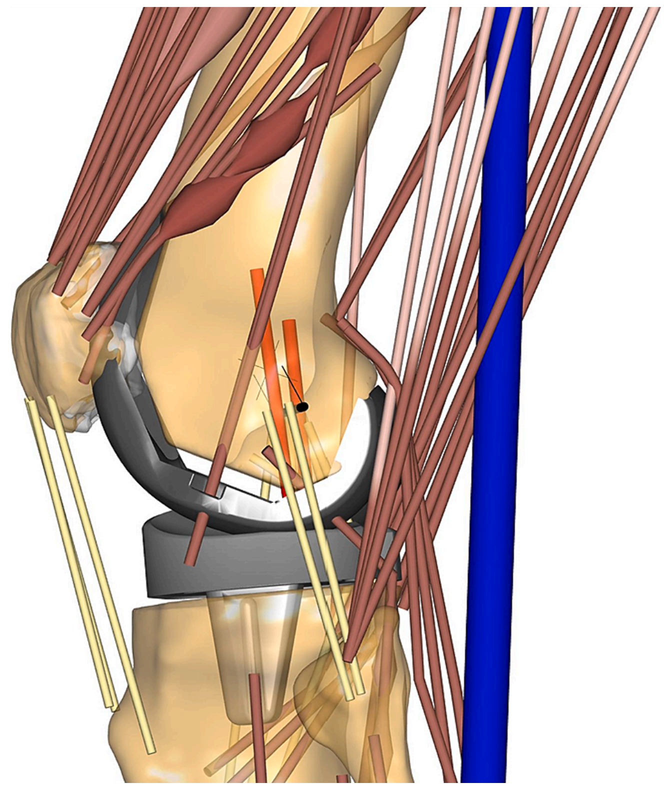

**Fig. 1.** Musculoskeletal model including femoral and tibial implant design of the current study.

while in clinical practice the outcome depends on patient factors such as age, gender and body weight index (BMI). For instance, several studies have investigated the influence of BMI on the outcomes of TKA (Başdelioğlu, 2020; Daniilidis et al., 2016; Wan et al., 2023). While there has been controversy on whether or not a high BMI negatively affects the primary fixation, a recent study has shown that a high BMI causes larger micromotions in reconstructions with metal implants (Wan et al., 2023). However, the influence of a high BMI on the primary fixation of a cementless PEEK femoral component is currently unknown. By adopting a population-based approach more insight can be gained into potential risk factors in patient populations.

Therefore, the research questions of this study were 1) What is the effect of simulated implant material change (PEEK vs. CoCr) on femoral micromotions within a population? 2) Is the primary fixation of a cementless femoral component influenced by patient characteristics (gender, age and BMI), and is there a difference in response as quantified by micromotions between PEEK and CoCr material?

## 2. Materials and methods

### 2.1. CT database

An anonymized CT database was created with approval from the ethical committee (reference number METC Oost-Nederland: 2021 – 13277). The patients were initially diagnosed with Kahler's disease. This patient category was selected as these patients undergo high resolution CT scans. The CT scans were checked and confirmed for not containing any pathologies in the knee joint. Gender, age, weight and height were known of these patients. As a result, 35 patients, and subsequently 70 femora, were included with the patient characteristics as listed in Table 1.

### 2.2. Workflow FE model

FE models were created of femoral TKA reconstructions, based on 70 femora. The models were analysed with femoral components simulating either PEEK or CoCr material properties, and were subjected to a gait and squat activity, resulting in 280 simulations. All models were analysed using MSC.Marc FE software (MSC.Marc2020, MSC. Software Corporation, Santa Ana, CA, USA). The models were created using an automated workflow, which is explained below in further detail.

1. Segmentation

The left and right femur of all patients were segmented and labelled from the CT scans using a convolutional neural network (https://grand-challenge.org/algorithms/femur-segmentation-in-ct/). The .mha files coming out of the segmentation algorithm were consecutively converted into surface meshes (.stl files).

2. Orientation of the femur and implant alignment

An anatomical reference frame was assigned to the surface meshes of the femur (Miranda et al., 2010). The femora were then aligned with the musculoskeletal model that was used to determine the implant-specific contact forces and centres of pressure of the loading conditions (see also "Boundary conditions, loads and contact interactions"). The CAD models of a generic cementless femoral component were available. At first, all implant sizes were rotated to replicate the implant orientation in the musculoskeletal model using a point cloud registration. The size of the femoral component for each specific femur was chosen based on the distance between the femoral anterior flange and the posterior condyles. The femur was then positioned such that overhang at the anterior flange and the posterior condyles was avoided. The implant was placed according to the mechanical alignment strategy.

3. Bone cuts

The simulated bone cuts were made based on the inner surface of the femoral component using modelling software (HyperMesh 2020, Altair Engineering, Troy, MI, USA). Additionally, the femur was cut on the proximal side at 120 mm from the joint line.

4. Volume meshing

The surface meshes of the femur and femoral component were converted into volume meshes consisting of tetrahedral elements (HyperMesh 2020, Altair Engineering, Troy, MI, USA). An edge length of 2.0 – 2.5 mm was used for both the femur and implant meshes, according to a previously performed mesh convergence study (Berahmani et al., 2016).

5. Bone material properties assignment

CT values were converted to bone mineral density values for each bone element using a previously published calibration method that uses the known Hounsfield unit intensities for air, fat and muscle (Eggermont et al., 2019). To allow for simulating permanent deformation of the bone during the virtual implantation, the bone was modelled as an elastic–plastic material, using a Von Mises yield material model (Keyak et al.,

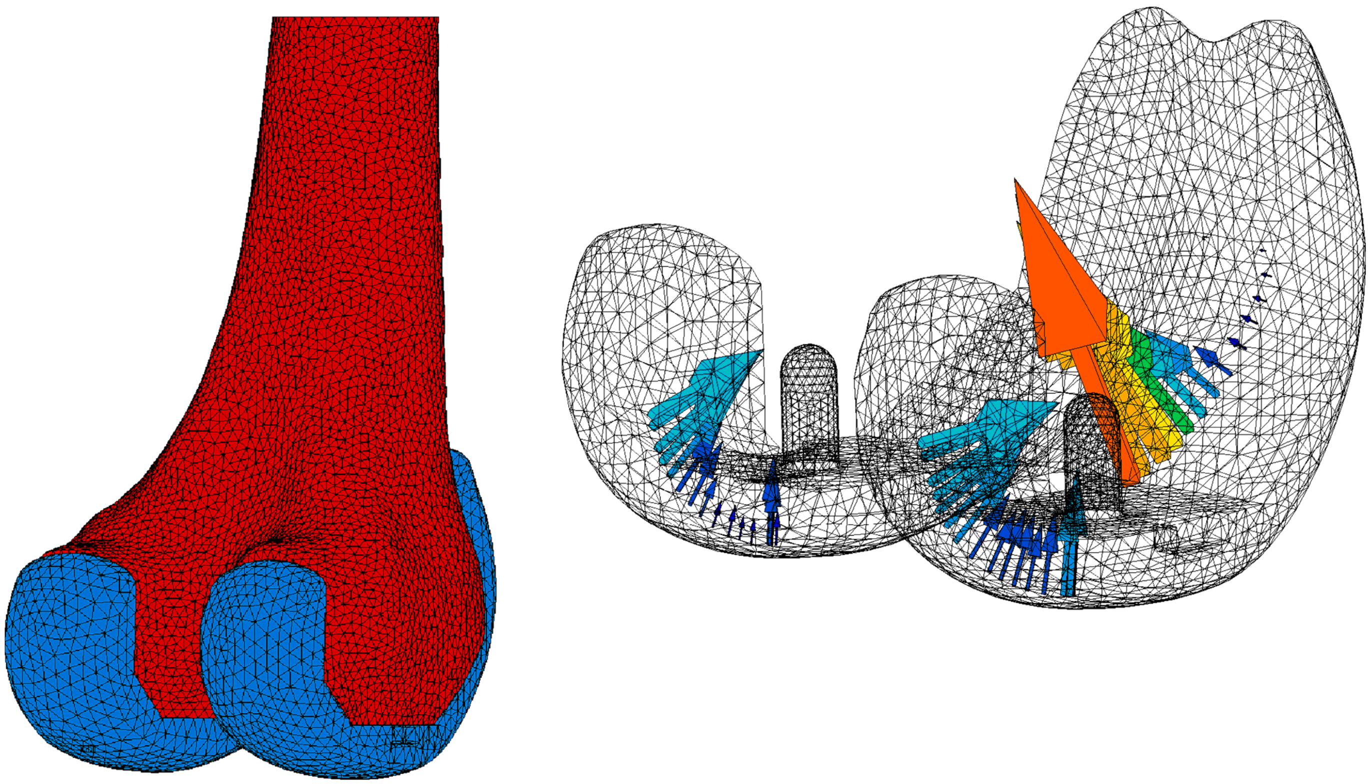

**Fig. 2.** Left: model of a right femur including femoral component. The model was fixated on the proximal side in all directions. Right: the medial and lateral tibiofemoral forces and the patellofemoral forces of a squat cycle are represented by the arrows. Larger arrows represent larger forces.

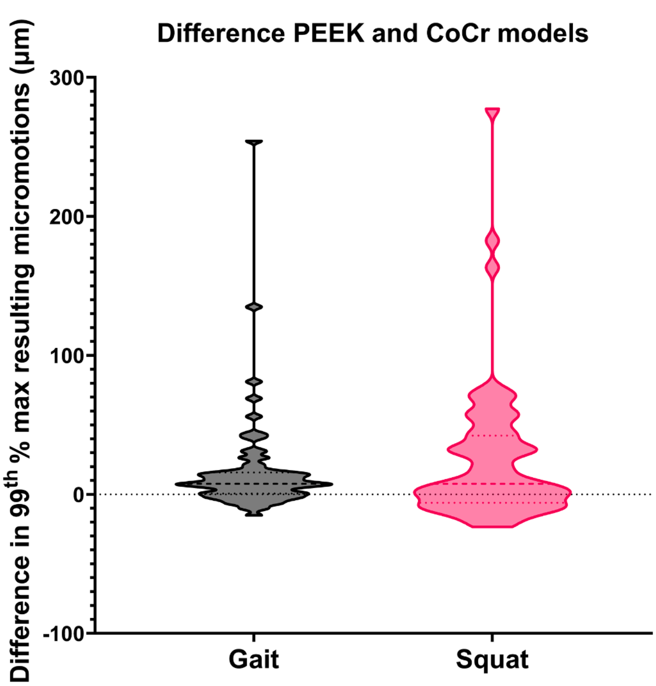


**Fig. 3.** Difference in the 99th percentile of the maximum resulting micromotions between the PEEK and CoCr models within all individual subjects of the population for the gait and squat models. Micromotion values for CoCr models were subtracted from PEEK model values for each specific model.

2005). The femoral component was modelled as an elastic isotropic material and assigned with the material properties of either PEEK (3.7 GPa) or CoCr (210 GPa).

6. Boundary conditions, loads and contact interactions

A single-sided touching algorithm was used to model the interaction between the femoral component and the femur. The friction between the femoral component and femur was modelled using a bilinear coulomb friction model. A coefficient of friction of 0.5 and an interference fit of 500 μm was applied at the anterior, posterior, distal and chamfer regions of the bone-implant interface and defined via the contact algorithm for material conditions (Post et al., 2022). The interference fit was linearly increased during a virtual implantation phase using 10 simulation increments until the maximum value of 500 μm was reached, during which plastic deformation of the bone was allowed. Subsequently, the interference fit was kept constant at its maximum value during the loading phase.

Implant-specific tibiofemoral and patellofemoral contact forces and centres of pressure of gait and squat activities were derived from a previously developed musculoskeletal model that was based on the Grand Challenge dataset (Marra et al., 2017). The musculoskeletal model was modified by incorporating the femoral and tibial implant design of the current study in the model (Fig. 1). The patella was included in the musculoskeletal model without a patellar button. The contact forces were scaled based on the patient's bodyweight and applied during four loading cycles to allow for (numerical) settling of the implant. One loading cycle consisted of 73 increments for the gait activity and 67 increments for the squat activity. Furthermore, the femur was fixated on the proximal side in all directions. An example of a model including femur and femoral component is showed in Fig. 2.

### 2.3. Outcome measures

The micromotions were defined as the relative displacements between the bone and the implant in the shearing direction using the same technique as Van der Ploeg et al. (van der Ploeg et al., 2012). More specifically, the motions of the contact nodes on the implant surface

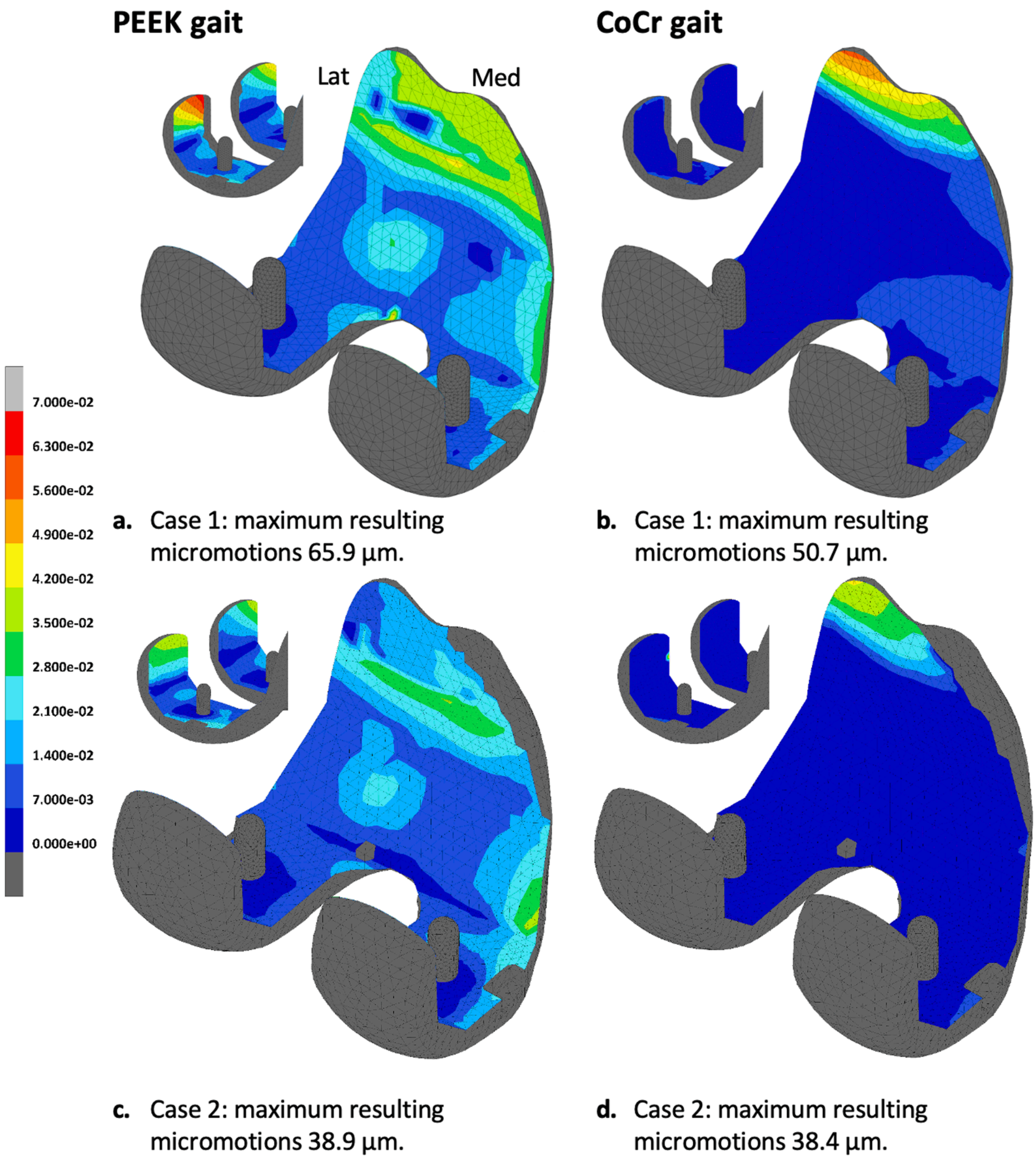


**Fig. 4.** Resulting micromotion distribution (mm) at the implant interface of the femoral component after the 4th loading cycle of a gait and squat activity. Case 1: Case with large maximum resulting micromotions within the population (man, left, 56 years, BMI 28.1 kg/m$^2$). Case 2: Case with average maximum resulting micromotions within the population (man, left, 73 years, BMI 26.6 kg/m$^2$). Case 3: Case with small maximum resulting micromotions within the population (woman, left, 54 years, BMI 18.6 kg/m$^2$).

were tracked relative to the contact faces of the bone surface. Each contact node on the implant surface was projected onto the closest contact face on the bone surface. The relative displacement of the contact node on the projected surface was calculated incrementally during the whole simulation. Regions with a large normal gap, for example due to overhang at the anterior flange, and regions of the pegs were excluded from the results. For each model, the resulting micromotions were defined as the largest distance during the full fourth loading cycle. The maximum resulting micromotion value was the maximum value of the contact nodes on the implant interface at a specific moment in time. The 99th percentile of the maximum resulting micromotions was taken to remove the nodes which potentially represented outliers. We analysed the 99th percentile of the maximum resulting micromotions visually via the distributions on the interface of the femoral component and quantitatively using violin plots. A violin plot shows the same information as boxplots (median, interquartile range and outliers), but also visualises the distribution of the data. Therefore, violin plots were used to visualize the difference in micromotions between the PEEK and CoCr models and to visualize the micromotions per patient characteristic.

### 2.4. Statistics

A linear mixed model was performed to evaluate statistical significance of the interactions between the micromotions, and the gender, age and BMI of the patients included in the population. Micromotion was taken as the dependent variable, and the fixed effects in our model included gender, age and BMI. The analysis was conducted using IBM SPSS Statistics 27. The results were presented as regression coefficient (β) and its 95 % confidence interval.

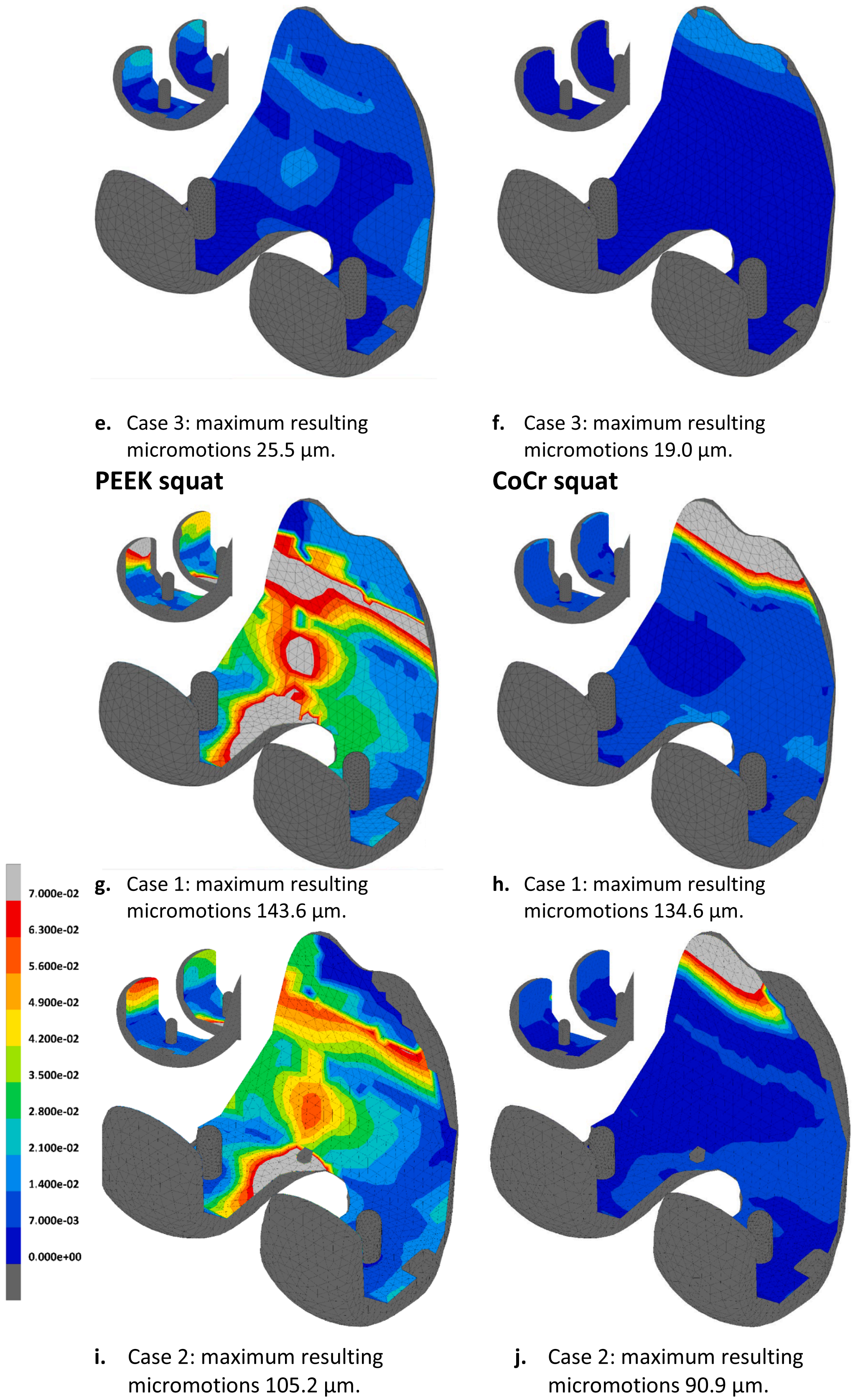


**Fig. 4.** (*continued*).

## 3. Results

16 simulations numerically failed to converge due to meshing errors that caused excessive deformations or inside-out elements and were therefore excluded from the data set. Subsequently, 264 of the 280 simulations (132 PEEK simulations and 132 CoCr simulations) were

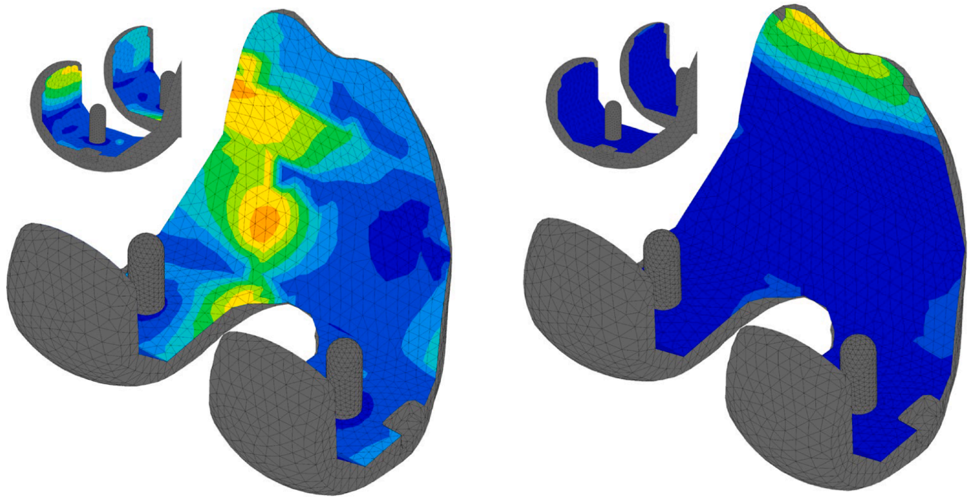

**k.** Case 3: maximum resulting micromotions 48.6 μm.

**l.** Case 3: maximum resulting micromotions 40.5 μm.

**Fig. 4.** (*continued*).

included in the analyses.

Overall, the PEEK models generated larger peak micromotions than the CoCr models (94.7 vs. 75.2 μm on average). For PEEK, the range of peak micromotions varied from 25.5 to 465.6 μm within the simulated cases, whereas for CoCr a range of 19.0 to 234.2 μm was found. Under the gait and squat load, some PEEK models generated slightly smaller peak micromotions than the CoCr models (Fig. 3).

Distinct differences were seen in the micromotion distributions between the PEEK and CoCr models for both the gait and squat models (Fig. 4). For the CoCr models, the largest micromotions were concentrated around the tip of the anterior flange, both during gait and squat loads (Fig. 4b, 4d, 4f, 4h, 4j and 4 l). The micromotions in the CoCr models were slightly larger during a squat load than during gait. In the PEEK models the largest resulting micromotions during gait were found at the anterior flange, medial distal region, chamfer regions and the posterior condyles (Fig. 4a, 4c and 4e). Under a squat load the largest resulting micromotions were found at the anterior flange, lateral regions of the chamfer and distal side and the posterior condyles (Fig. 4g, 4i and 4k). Hence, micromotions were greater at the tip of the anterior flange in the CoCr models, while the PEEK models displayed greater micromotions in other regions. While the distribution of the micromotions over the implant surfaces was quite consistent for the PEEK and CoCr models, there were distinct differences between specific cases. Fig. 4 shows micromotion distributions for three cases with a PEEK and CoCr implant with various maximum micromotion values, illustrating the inter-specimen variations seen within the population of models. These results show relatively high micromotions in the notch area for the PEEK models and at the flange area for the CoCr models (Fig. 4).

The micromotions of all femoral models significantly increased with BMI: 3.843 ± 0.600 μm (95 % CI: 2.662, 5.024) ($P < 0.001$). Neither gender nor age of the patients had a significant effect on the micromotions of all femoral models. There was no clinically relevant difference in response to BMI between the PEEK and CoCr material properties (Fig. 5).

## 4. Discussion

In this study we studied the effect of implant material (PEEK vs. CoCr) on femoral micromotions within a population, and investigated the effect of patient characteristics (gender, age and BMI) on these micromotions. The current results show that, within the studied population, the micromotions of a cementless component generally increased when changing the material properties from CoCr to PEEK. Furthermore, the locations of peak micromotions were clearly different between the PEEK and CoCr models. Although the magnitudes of the micromotions were affected by specific bone cases, the distributions of the micromotion patterns were similar and consistent among the cases included in this study showing relatively high micromotions in the notch area for the PEEK models and at the flange area for the CoCr models. Of the included patient characteristics, only BMI had a significant effect on micromotions in both the CoCr and PEEK models.

The overall current finding that PEEK material led to larger micromotions is in agreement with an earlier study in which the effect of material properties (simulating either PEEK or CoCr) of a cementless femoral component were compared in a single model, with parametric variations (Post et al., 2022). In that single model study, the maximum micromotion was 70.1 μm and 15.2 μm for a PEEK and CoCr material, respectively, compared to a median maximum micromotion of 94.7 vs. 75.2 μm in the current study. However, the current study also found some gait and squat models with larger values for the CoCr component than the PEEK component, which emphasizes the importance of including a larger patient population, with more variability, to obtain a more robust outcome of a computational study. Additionally, this study found that the distributions of the micromotions were different for the PEEK models as compared to the CoCr models, which is in contrast with the single-model study. This can be explained by the differences in the loading configurations between the two studies (Orthoload vs. a dedicated musculoskeletal model) and type of activity (jogging vs. gait and squat) that were modelled. The use of implant-specific loading conditions including the patellofemoral forces is therefore important in the investigation of the primary fixation of a cementless PEEK femoral component. Although the maximum micromotions were somewhat higher in the PEEK models, the majority of the implant surface displayed micromotions that were below the threshold of 40 μm for bone ingrowth (Engh et al., 1992). Moreover, the actual threshold for osseointegration has been subject of debate, and has been suggested to possibly be as high as 112 μm, based on a systematic review by Kohli et al. (Kohli et al., 2021). This suggests that also for a PEEK femoral component a large portion of the implant-bone interface has favourable conditions for osseointegration and long-term implant fixation. In addition, while it is

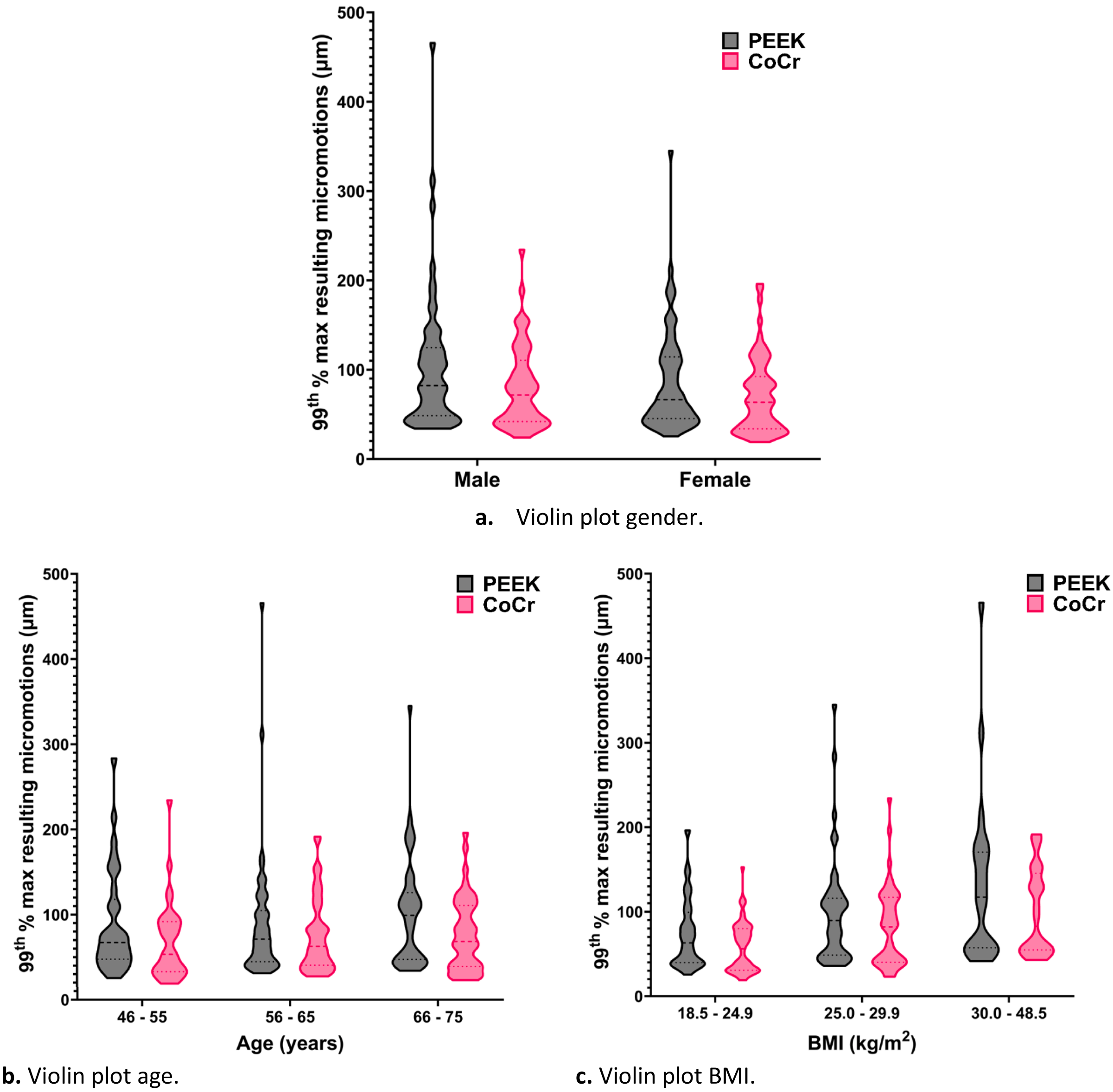


**Fig. 5.** Violin plots of gender, age and BMI.

obvious from clinical practice that fixation of CoCr femoral components is quite successful, the optimal conditions for implant osseointegration are largely unknown, which makes extending the current computational results to clinical practice challenging.

The optimal circumstances for osseointegration include both biomechanical and biological circumstances. From a biological point of view parameters of importance are good vascularisation, availability of stem cells and appropriate surface properties (porosity and coatings) that stimulate bone apposition. From a mechanobiological point of view biomechanical stimuli such as suggested by Prendergast et al. suggest that 1) low fluid flow and 2) low shearing strains of the newly formed bone, stimulate bone formation (Prendergast et al., 1997). It is likely that these two quantities are related to micromotions as determined in this study, i.e. high micromotions are likely to increase fluid flow and shearing stresses at the interface.

Furthermore, ingrowth of a prosthetic component after implantation is a gradual biological process and bony ingrowth will progressively fixate the implant. Retrieved specimens show that ingrowth can be quite regional and incomplete (Hanzlik et al., 2013; Hanzlik et al., 2015). Hence, it may be that it is more important to assess whether there are regions of the implant where bone ingrowth will be initiated rather than focussing on peak micromotions as done in this study. Considering the micromotion distributions found in the population cases, low-micromotion areas were found in all cases, independent of the simulated implant material, suggesting appropriate biomechanical conditions to initiate the bone ingrowth process.

The current study furthermore investigated the effect of patient characteristics on primary fixation. From all characteristics, only BMI had a significant effect on the micromotions, with micromotions increasing with BMI. In line with our study, Wan et al. concluded that a high BMI causes higher micromotions in both a gait and deep knee bend activity (Wan et al., 2023). On the influence of gender and age on the primary fixation of cementless femoral components is currently not much known. Gibbons et al. studied the risk of implant subsidence in elderly women who are more at risk for osteoporosis (Gibbons et al., 2023), and found no increased risk in this patient population. In our study, we also did not find a relation with elderly women and higher risk of large micromotions. However, it is expected that the reduced bone quality in this patient group would have an influence on the primary fixation of cementless femoral components. A more extensive population-based study including information on the bone quality of the femurs would therefore be required. Additional research is furthermore required to elucidate the relation between implant stiffness and primary fixation, and whether there is an optimal stiffness that provides a good balance between primary fixation and long-term effects such as stress shielding.

It should be noted that there are a number of limitations of this study that affect interpretation of the results. As described above, the first limitation is related to the description of the bone quality in this study. While the patient-specific bone density distribution was incorporated in the FE models, a single parameter describing the overall bone quality, that can be used as a comparison within the studied population, was lacking, restricting statistical analysis of the effect of the overall bone quality on primary fixation. A second limitation is related to the missing values due to simulations that did not converge. Numerical none-convergence could be related to the (numerical) instability at the bone-implant interface, suggesting that circumstances that decrease stability would lead to more none-converged cases. However, we could not find any clear indications (e.g. like lower elastic moduli of bone or implant) that could explain the numerical instability of the cases. Another limitation of this study is the limited number of cases included. While this population study is a first start in the analysis of the influence of patient characteristics on the primary fixation of cementless femoral components, a larger study is required for the analysis of the outliers which may provide more detailed information on specific risk factors for patients receiving a TKA. Additionally, although we did incorporate plasticity of the bone during implant insertion, we did not include viscoelastic behaviour of the bone, while this may have an influence on the compressive forces generated by the interference fit. Another point to raise is the fact that this FE study was a parametric study; the material properties of the simulated component geometry were allocated with either CoCr or PEEK elastic properties and the effect on initial fixation assessed. In reality, a PEEK component will be provided with an ingrowth surface, typically made by titanium, which could increase overall stiffness. This could have an effect on the initial fixation of the component, but was not taken into account in the current study. Also, a single implant alignment strategy was adopted, while variations in alignment may lead to differences in the loading configuration, possibly affecting micromotions at the implant-bone interface. Lastly, the models simulated in our study were generated with a nominal implant-bone interface, while surgical cuts that can occur in clinical practice may influence the primary fixation of cementless femoral components, leaving gaps at the interface and creating less optimal conditions for bone ingrowth.

In conclusion, the current population study gives insights into the primary fixation and its variation of a cementless femoral component in a cohort of computational models with varying patient characteristics. Although the distributions of the micromotions were similar within this population, the differences in micromotion magnitudes were observed amongst the cases. PEEK models generated larger maximum micromotions than the CoCr models (94.7 vs. 75.2 μm, respectively) except for a few gait and squat models. BMI was a significant parameter in the primary fixation of cementless femoral components. The results indicate that implant-specific loading conditions, including the patellofemoral forces, are essential for testing a cementless PEEK femoral component.

Future work will focus on a more in-depth multivariate analysis to investigate the effect of interactions of patient characteristics, including bone quality, and implant fixation. Moreover, an outlier analysis of a larger population may provide more insights in potential risk factors in patient characteristics for the primary fixation of cementless femoral components.

## CRediT authorship contribution statement

**Corine E. Post:** . **Thom Bitter:** Writing – review & editing, Supervision, Methodology, Conceptualization. **Adam Briscoe:** Writing – review & editing, Resources, Conceptualization. **René Fluit:** Writing – review & editing, Conceptualization. **Nico Verdonschot:** Writing – review & editing, Supervision, Resources, Funding acquisition, Conceptualization. **Dennis Janssen:** Writing – review & editing, Supervision, Resources, Methodology, Funding acquisition, Conceptualization.

## Declaration of competing interest

The authors declare the following financial interests/personal relationships which may be considered as potential competing interests: A. B. is a paid employee of Invibio Ltd. and had a role in the study design and review of the manuscript. N.V. is a paid consultant for Invibio Ltd. D.J. is a paid consultant for Invibio Ltd and receives research support as a principal investigator from Invibio Ltd. The other authors declare no conflict of interest.

## Acknowledgements

This study was funded by Invibio Ltd., Lancashire, United Kingdom. Invibio Ltd. was not involved in the collection, analysis and interpretation of the data. No writing assistance was provided for writing this manuscript. The authors would like to thank Thomas Hoogeboom for his assistance in performing the statistical analyses.

## References

Başdelioğlu, K., 2020. Effects of body mass index on outcomes of total knee arthroplasty. Eur. J. Orthop. Surg. Traumatol. 31 (3), 595–600. https://doi.org/10.1007/s00590-020-02829-6.

Berahmani, S., Janssen, D., Wolfson, D., de Waal Malefijt, M., Fitzpatrick, C.K., Rullkoetter, P.J., Verdonschot, N., 2016. FE analysis of the effects of simplifications in experimental testing on micromotions of uncemented femoral knee implants. J. Orthop. Res. 34 (5), 812–819. https://doi.org/10.1002/jor.23074.

Daniilidis, K., Yao, D., Gosheger, G., Berssen, C., Budny, T., Dieckmann, R., Holl, S., 2016. Does BMI influence clinical outcomes after total knee arthroplasty? Technol. Health Care 24 (3), 367–375. https://doi.org/10.3233/THC-151128.

de Ruiter, L., Janssen, D., Briscoe, A., Verdonschot, N., 2017. A preclinical numerical assessment of a polyetheretherketone femoral component in total knee arthroplasty during gait. J Exp Orthop 4 (1), 3. https://doi.org/10.1186/s40634-017-0078-4.

Eggermont, F., Verdonschot, N., van der Linden, Y., Tanck, E., 2019. Calibration with or without phantom for fracture risk prediction in cancer patients with femoral bone metastases using CT-based finite element models. PLoS One 14 (7), e0220564.

Engh, C.A., O'Connor, D., Jasty, M., McGovern, T.F., Bobyn, D., Harris, W.H., 1992. Quantification of implant micromotion, strain shielding, and bone resorption with porous-coated anatomic Medullary locking femoral prostheses. Clin. Orthop. Relat. Res. 285, 13–29.

Gibbons, J.P., Cassidy, R.S., Bryce, L., Napier, R.J., Bloch, B.V., Beverland, D.E., 2023. Is cementless Total knee arthroplasty safe in women over 75 Y of age? J. Arthroplasty 38 (4), 691–699. https://doi.org/10.1016/j.arth.2022.10.021.

Hanzlik, J. A., Day, J. S., & Acknowledged Contributors: Ingrowth Retrieval Study, G. (2013). Bone ingrowth in well-fixed retrieved porous tantalum implants. *J Arthroplasty*, *28*(6), 922-927. DOI: 10.1016/j.arth.2013.01.035.

Hanzlik, J. A., Day, J. S., Rimnac, C. M., Kurtz, S. M., & Ingrowth retrieval study, g. (2015). Is There A Difference in Bone Ingrowth in Modular Versus Monoblock Porous Tantalum Tibial Trays? *J Arthroplasty*, *30*(6), 1073-1078. DOI: 10.1016/j.arth.2015.01.010.

Hofmann, A.A., Bloebaum, R.D., Bachus, K.N., 1997. Progression of human bone ingrowth into porous-coated implants. rate of bone ingrowth in humans. Acta Orthop. Scand. 68 (2), 161–166. https://doi.org/10.3109/17453679709004000.

Keyak, J.H., Kaneko, T.S., Tehranzadeh, J., Skinner, H.B., 2005. Predicting proximal femoral strength using structural engineering models. Clin. Orthop. Relat. Res. 437, 219–228. https://doi.org/10.1097/01.blo.0000164400.37905.22.

Kohli, N., Stoddart, J.C., van Arkel, R.J., 2021. The limit of tolerable micromotion for implant osseointegration: a systematic review. Sci. Rep. 11 (1), 10797. https://doi.org/10.1038/s41598-021-90142-5.

Marra, M.A., Andersen, M.S., Damsgaard, M., Koopman, B.F.J.M., Janssen, D., Verdonschot, N., 2017. Evaluation of a surrogate contact model in force-dependent kinematic simulations of Total knee replacement. J. Biomech. Eng. 139 (8) https://doi.org/10.1115/1.4036605.

Miranda, D.L., Rainbow, M.J., Leventhal, E.L., Crisco, J.J., Fleming, B.C., 2010. Automatic determination of anatomical coordinate systems for three-dimensional bone models of the isolated human knee. J. Biomech. 43 (8), 1623–1626. https://doi.org/10.1016/j.jbiomech.2010.01.036.

Nishio, F., Morita, K., Doi, K., Kato, M., Abekura, H., Yamaoka, H., Kakimoto, N., Tsuga, K., 2023. Radiopaque properties of polyetheretherketone crown at laboratory study. J. Oral Biosci. 65 (3), 253–258. https://doi.org/10.1016/j.job.2023.05.002.

Post, C.E., Bitter, T., Briscoe, A., Verdonschot, N., Janssen, D., 2022. A FE study on the effect of interference fit and coefficient of friction on the micromotions and interface gaps of a cementless PEEK femoral component. J. Biomech. 137, 111057 https://doi.org/10.1016/j.jbiomech.2022.111057.

Prendergast, P.J., Huiskes, R., Soballe, K., 1997. Biophy sical stimuli on cells during tissue differentiation at implant interfaces. J. Biomech. 30, 539–548. https://doi.org/10.1016/s0021-9290(96)00140-6.

Rankin, K.E., Dickinson, A.S., Briscoe, A., Browne, M., 2016. Does a PEEK femoral TKA implant preserve intact femoral Surface strains Compared with CoCr? a Preliminary laboratory study. Clin. Orthop. Relat. Res. 474 (11), 2405–2413. https://doi.org/10.1007/s11999-016-4801-8.

van der Ploeg, B., Tarala, M., Homminga, J., Janssen, D., Buma, P., Verdonschot, N., 2012. Toward a more realistic prediction of peri-prosthetic micromotions. J. Orthop. Res. 30 (7), 1147–1154. https://doi.org/10.1002/jor.22041.

Wan, Q., Zhang, A., Liu, Y., Chen, H., Zhang, J., Xue, H., Han, Q., Wang, J., 2023. The influence of body weight index on initial stability of uncemented femoral knee protheses: a finite element study. Heliyon 9 (3), e13819.